0022-3565/09/3292-459–468$20.00
THE JOURNAL OF PHARMACOLOGY AND EXPERIMENTAL THERAPEUTICS
JPET 329:459–468, 2009

Vol. 329, No. 2
150094/3463230
Printed in U.S.A.

Procognitive and Neuroprotective Activity of a Novel α7 Nicotinic Acetylcholine Receptor Agonist for Treatment of Neurodegenerative and Cognitive Disorders

Renza Roncarati, Carla Scali, Thomas A. Comery, Steven M. Grauer, Suzan Aschmi, Hendrick Bothmann, Brian Jow, Dianne Kowal, Marco Gianfriddo, Cody Kelley, Ugo Zanelli, Chiara Ghiron, Simon Haydar, John Dunlop, and Georg C. Terstappen

Siena Biotech S.p.A., Siena, Italy (R.R., C.S., H.B., M.G., U.Z., C.G., G.C.T.); and Discovery Neuroscience Wyeth Research, Princeton, New Jersey (T.A.C., S.M.G., S.A., B.J., D.K., C.K., S.H., J.D.)

Received December 22, 2008; accepted February 13, 2009

ABSTRACT

The α7 nicotinic acetylcholine receptor (nAChR) is a promising target for treatment of cognitive dysfunction associated with Alzheimer's disease and schizophrenia. Here, we report the pharmacological properties of 5-morpholin-4-yl-pentanoic acid (4-pyridin-3-yl-phenyl)-amide [SEN12333 (WAY-317538)], a novel selective agonist of α7 nAChR. SEN12333 shows high affinity for the rat α7 receptor expressed in GH4C1 cells (K_i = 260 nM) and acts as full agonist in functional Ca^{2+} flux studies (EC_{50} = 1.6 μM). In whole-cell patch-clamp recordings, SEN12333 activated peak currents and maximal total charges similar to acetylcholine (EC_{50} = 12 μM). The compound did not show agonist activity at other nicotinic receptors tested and acted as a weak antagonist at α3-containing receptors. SEN12333 treatment (3 mg/kg i.p.) improved episodic memory in a novel object recognition task in rats in conditions of spontaneous forgetting as well as cognitive disruptions induced via glutamatergic [5*H*-dibenzo[*a*,*d*]cyclohepten-5,10-imine (dizocilpine maleate); MK-801] or cholinergic (scopolamine) mechanisms. This improvement was blocked by the α7-selective antagonist methyllycaconitine, indicating that it is mediated by α7 activation. SEN12333 also prevented a scopolamine-induced deficit in a passive avoidance task. In models targeting other cognitive domains, including attention and perceptual processing, SEN12333 normalized the apomorphine-induced deficit of prepulse inhibition. Neuroprotection of SEN12333 was demonstrated in quisqualate-lesioned animals in which treatment with SEN12333 (3 mg/kg/day i.p.) resulted in a significant protection of choline acetyltransferase-positive neurons in the lesioned hemisphere. Cumulatively, our results demonstrate that the novel α7 nAChR agonist SEN12333 has procognitive and neuroprotective properties, further demonstrating utility of α7 agonists for treatment of neurodegenerative and cognitive disorders.

The family of nicotinic acetylcholine receptors, which comprises 16 different subunits in human (α1–7, α9–10, β1–4, δ, ε, and γ) that can form many functional homo- and heteropentameric receptor ion channel combinations, contributes to cholinergic neurotransmission in the nervous system and at the neuromuscular junction. The α7 nicotinic acetylcholine receptors (nAChRs) are rapidly desensitizing ligand-gated ion channels that are abundantly expressed in the cerebral cortex and the hippocampus, a limbic structure intimately linked to attention processing and memory formation (Gotti et al., 2006). In the hippocampus, α7 nAChRs are present in interneurons and glutamatergic pyramidal neurons, in which they are localized presynaptically in nerve terminals and postsynaptically in dendritic spines and soma. In line with their localization, α7 nAChRs modulate neurotransmitter release and are responsible for direct fast excitatory neuro-

Article, publication date, and citation information can be found at http://jpet.aspetjournals.org.
doi:10.1124/jpet.108.150094.

ABBREVIATIONS: nAChR, nicotinic acetylcholine receptor; AD, Alzheimer's disease; SEN12333, 5-morpholin-4-yl-pentanoic acid (4-pyridin-3-yl-phenyl)-amide; MK-801, 5*H*-dibenzo[*a*,*d*]cyclohepten-5,10-imine (dizocilpine maleate); MLA, methyllycaconitine; PPI, prepulse inhibition; HEK, human embryonic kidney; 5-HT, 5-hydroxytryptamine; FLIPR, fluorometric imaging plate reader; hERG, human *ether-a-go-go*-related gene; PBS, phosphate-buffered saline; LC-MS/MS, high-performance liquid chromatography in combination with mass spectrometry; T, trial; F, familiar; N, novel; ANOVA, analysis of variance; LSD, least significant difference; NBM, nucleus basalis magnocellularis; ChAT, choline acetyltransferase; DAB, 3,3′-diaminobenzidine; ACh, acetylcholine; AUC, area under the curve; SSR-180711, 1,4-diazabicyclo[3.2.2]nonane-4-carboxylic acid, 4-bromophenyl ester; r, rat; h, human; PNU-282987, *N*-[(3*R*)-1-azabicyclo[2.2.2]oct-3-yl]-4-chlorobenzamide hydrochloride; PHA-709829, *N*-[(3*R*,5*R*)-1-azabicyclo[3.2.1]oct-3-yl]furo[2,3-c]pyridine-5-carboxamide; AR-R17779, (−)-spiro[1-azabicyclo[2.2.2]octane-3,5′-oxazolidin-2′-one].

transmission (Frazier et al., 1998; Alkondon et al., 2000; Fabian-Fine et al., 2001; Marchi et al., 2002).

Several lines of evidence indicate that attention and cognitive impairments, which are characteristic of a variety of neurological and psychiatric disorders such as Alzheimer's disease (AD) and schizophrenia, may involve degeneration or hypofunction of cholinergic input that originates from the septum. In studies of the expression of α7 nAChRs in AD brain both, increased and decreased levels of expression were observed, which can either be ascribed to a compensatory response to maintain basocortical cholinergic activity during AD progression or to opposite changes in neurons and astrocytes, respectively (Court et al., 2001; Teaktong et al., 2003; Gotti and Clementi, 2004; Yu et al., 2005; Counts et al., 2007). Reduced expression levels of α7 nAChRs have also been observed in brains from schizophrenic patients (Freedman et al., 2000). Moreover, genetic linkage has identified α7 nAChRs as a predisposing factor related to sensory gating deficits (Stassen et al., 2000; Gault et al., 2003), which is a hallmark of schizophrenia and also present in AD patients (Jessen et al., 2001). Taken together, these findings provide compelling evidence for a role of α7 nAChRs in these pathologies and suggest that specific activation of α7 nAChRs may represent a therapeutic strategy for ameliorating cognitive deficits associated with neurodegenerative and neuropsychiatric diseases. In agreement with this hypothesis, the prototypical nAChR agonist nicotine, as well as more selective α7 agonists described more recently, has been shown to improve cognitive performance in animal models and humans (Newhouse et al., 2004; Van Kampen et al., 2004; Hajós et al., 2005; Pichat et al., 2007). Several reports also suggest that α7 nAChRs mediate protection against neurotoxicity induced by amyloid β and excitotoxic insults (Kihara et al., 2001; O'Neill et al., 2002; Hellström-Lindahl et al., 2004; Hu et al., 2007).

Here, we report the in vitro and in vivo properties of the novel α7 nAChR agonist SEN12333 (Fig. 1), which was investigated in several rodent models of relevance for symptoms present in demented and schizophrenic patients (e.g., cognition, attention, and perceptual processing). SEN12333 was evaluated for its potential to compensate glutamatergic- or cholinergic-induced deficits in a novel object recognition task of episodic memory as well as in a passive avoidance test of working memory. Normalization of sensory gating deficits was studied in an apomorphine-induced prepulse inhibition-disruption model. Finally, the neuroprotective potential of SEN12333 was analyzed in a model of cholinergic degeneration induced by quisqualic acid injection in the nucleus basalis magnocellularis followed by identification of surviving cholinergic neurons.

Materials and Methods

Drugs. SEN123333 was synthesized by Siena Biotech S.p.A. (Siena, Italy). Dose calculations were based on the active moiety. Scopolamine, apomorphine, MK-801, quisqualic acid, Tween 80, and methylcellulose were obtained from Sigma-Aldrich (St. Louis, MO). Methyllycaconitine (MLA) was obtained from Tocris Bioscience (Bristol, UK). Drugs were dissolved in saline, 2% Tween 80, and 0.5% methylcellulose. All other materials were analytical grade and were purchased from Aldrich Chemical Co. (Milwaukee, WI) and Sigma-Aldrich (Milan, Italy) if not stated otherwise.

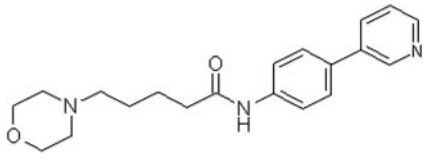

Fig. 1. Chemical structure of SEN12333 (WAY-317538).

Animals for in Vivo Pharmacology. Male Wistar rats (Harlan, Milan, Italy) were used in all studies except MK-801-induced object recognition deficit and prepulse inhibition (PPI) tests in which male Long Evans rats (Charles River, Calco, Italy) were used. For all behavioral studies, rats were 3 months old and weighed 250 to 350 g. Both rat strains are well suited and have extensively been used for behavioral/cognitive studies. Use of different strains for different tests in this study reflects prior investigator expertise with the respective animal model/strain. Rats were housed in macrolon cages with ad libitum food and water and maintained on a 12-h light/dark cycle at 23°C room temperature. All experiments were carried out according to the guidelines of the European Community's Council for Animal Experiments (86/609/EEC) and the Principles of Laboratory Animal Care as adopted and promulgated by the National Institutes of Health (publication 85-23, 1985). All efforts were made to minimize the number of animals used and their suffering.

Ca^{2+} Flux and Membrane Potential Measurements with an FLIPR System. The following recombinant cell lines were used as specific sources of receptors: GH4C1 cells stably transfected with pCEP4/rat α7 nAChR as described previously (Dunlop et al., 2007); HEK293 cell lines stably expressing human α4β2 nAChR (obtained from J. Lindstrom, The University of Pennsylvania, Philadelphia, PA) or 5-hydroxytryptamine (5-HT_{3A} receptors (Dunlop et al., 2007). Native neuroblastoma SH-SY5Y cells were used as source of human ganglionic nAChRs (α3), and TE671 rhabdomyosarcoma cells were used as endogenous source of muscle α1β1δγ receptors. GH4C1 cells expressing α7 and HEK293 cells expressing 5-HT_{3A} receptors were analyzed by Ca^{2+} flux measurements using a fluorometric imaging plate reader system (FLIPR; Molecular Devices, Sunnyvale, CA), whereas the cells expressing the nicotinic receptor subunits α1, α3, and α4 were tested in the FLIPR system with a membrane potential-sensitive dye.

For Ca^{2+} flux analysis, cells were plated in 96-well, clear-bottomed, poly-D-lysine-coated black microtiter plates (Corning Life Sciences, Lowell, MA) at a density of 1×10^5 cells/well for α7-expressing GH4C1 cells or 8×10^4 cells/well for 5-HT_{3A}-expressing HEK293 cells and cultured for 24 h before experiments. The medium was then replaced with 100 μl of Hanks' balanced salt solution-20 mM HEPES, pH 7.4 (assay buffer), containing 4 μM Fluo-4-acetoxymethyl ester, 0.02% Pluronic acid, and 5 mM probenecid. After 40 min of incubation at 37°C, the labeling solution was replaced with 200 μl of assay buffer containing 2.5 mM probenecid. Plates were then transferred to the FLIPR system. Compounds to be tested were prepared in assay buffer as 5 times concentrated solutions in a separate 96-well polypropylene plate. Basal fluorescence was recorded for 30 s, followed by addition of 50 μl of test compound (to assess agonist activity; first addition). Measurements were made at 1-s intervals for 1 min, followed by measurements every 30 s for 10 min. Subsequently, for the second addition for α7-expressing GH4C1 cells, nicotine (final concentration, 10 μM) was added to each well except negative controls (to assess positive modulation and antagonism of nicotine response). For testing 5-HT_{3A} receptors, chlorophenylbiguanide (final concentration, 1 μM) was added to each well except negative controls. Measurements were made at 1-s intervals for 1 min after the second addition and at 3-s intervals for the remaining 3 min. Results were exported from the FLIPR raw data as maximum-minimum of fluorescence signal intensity in two intervals corresponding to the first and the second addition of compounds. The responses were normalized to the positive control, and EC_{50} and IC_{50} values were calculated using Xlfit version 4.2 (Microsoft, Redmond, WA) with a sigmoidal concentration response (variable slope) accord-

ing to the equation Y = bottom + (top − bottom)/(1 + (EC_{50}/X)$\hat{H}$ill slope), where X is the concentration, Y is the response, bottom is the bottom plateau of the curve, and top is the top plateau. Assay performance was robust as reflected by a Z′ factor >0.6.

Activity of compounds at the muscle- and ganglionic-type nAChR receptors was determined using a membrane potential-sensitive fluorescence dye. TE671 and SHSY5Y cells were plated at a density of 5×10^4 cells/well 24 h before assay. Growth media were removed from the cells, and membrane potential dye (Molecular Devices), reconstituted in Hanks' balanced salt solution 5 times more diluted compared with the manufacturer's instructions, was added to the wells. Plates were incubated for 60 min at room temperature and then directly transferred to the FLIPR system. Compounds to be tested were prepared in assay buffer as 5 times concentrated solutions in a separate 96-well polypropylene plate. Baseline fluorescence was monitored for the first 10 s followed by the addition of compounds. For detection of antagonists or positive allosteric modulator activity, agonist (epibatidine; final concentration, 1 μM) was added to every well except negative controls. Signal recordings were performed as described above. Results were exported from the FLIPR raw data as sum of fluorescence signal intensity for the first addition and maximum-minimum for the second addition of compounds. The responses were normalized to the positive control (epibatidine; final concentration, 1 μM), and EC_{50} values were calculated as described above.

Electrophysiology. GH4C1 cells stably expressing rat α7 nAChR were treated with 0.5 mM sodium butyrate added to the medium for 2 days before patch-clamp recordings. Patch pipets had resistances of ~7 MOhm when filled with 5 mM EGTA, 120 mM potassium gluconate, 5 mM KCl, 10 mM HEPES, 5 mM K_2ATP, 5 mM Na_2-phosphocreatine, 1 mM $CaCl_2$, and 2 mM $MgCl_2$. Cells were voltage-clamped at −60 mV with an EPC-9 amplifier (HEKA, Lambrecht/Pfalz, Germany). To measure the fast activation and desensitization of α7 current, the Dynaflow (Cellectricon, Gaithersburg, MD) fast perfusion system with 16- or 48-well chips was used. Different concentrations of acetylcholine (ACh) or SEN12333 were applied to cells in between washes with bath solution (Hanks' balanced salt solution + 10 mM HEPES). Data were acquired at 1 kHz for 2-s episodes (500 ms for bath, 500 ms for agonist, and 1000 ms for wash), with a 10-s interval between episodes. Peak current amplitude and total charge (area under the curve) were measured with the HEKA Pulse program. Concentration-response curves and EC_{50} values were plotted and calculated with Origin (OriginLab Corp., Northampton, MA).

Radioligand Binding Assay. [^{3}H]Epibatidine binding studies were performed as described previously (Dunlop et al., 2007). Briefly, cell membrane preparations derived from GH4C1 cells stably expressing rat α7 nAChRs were suspended in binding buffer (50 mM HEPES, pH 7.4, 3 mM KCl, 70 mM NaCl, and 10 mM $MgCl_2$), 5 nM [^{3}H]epibatidine (specific activity, 53 Ci/mmol; GE Healthcare, Chalfont St. Giles, Buckinghamshire, UK) and SEN12333 to achieve a final volume of 200 μl in a 96-well polypropylene plate. Nicotine at 300 μM was used for determination of nonspecific binding. After incubation at room temperature (23°C) for 1 h, samples were rapidly filtered through Unifilter GF/B filters using a Filtermate (PerkinElmer Life and Analytical Sciences, Boston, MA) and washed five times with ice-cold binding buffer. Samples were processed and counted for radioactivity using a TopCount NXT microplate luminescence and scintillation counter (PerkinElmer Life and Analytical Sciences). Competition binding curves were fitted with a four-parameter logistic model. K_i values were calculated by the Cheng-Prusoff equation using the GraphPad Prism software package (GraphPad Software Inc., San Diego, CA).

Receptor Selectivity and hERG Activity. Interaction of SEN12333 with ~70 binding sites, including all major classes of neurotransmitters, growth factors, and peptide receptors, was examined at 10 μM concentration (Novascreen; Caliper Biosciences, Hopkinton, MA), including a histamine-3 binding assay with [^{3}H]*N*-α-methylhistamine as radioligand and rat forebrain tissue. Functional antagonist activity at histamine-3 receptor was determined in a recombinant HEK293 cell line stably expressing the receptor. In brief, cells were resuspended in PBS with 500 μM isobutylmethylxanthine. Two thousand cells per well were incubated with 1 μM histamine plus 10 μM forskolin plus various concentrations of SEN12333 in a total volume of 30 μl in 384-well plates for 30 min at 30°C. Final test compound concentrations ranged from 10^{-4} to 10^{-10} M. Cyclic AMP levels were measured using HitHunter cAMP kit (DiscoveRx, Fremont, CA) according to manufacturer's instructions and by chemiluminescence detection using a TopCount liquid scintillation counter (PerkinElmer Life and Analytical Sciences). Cyclic AMP levels in control cells receiving10 μM forskolin plus 1 μM histamine are considered 0%, and in cells receiving 10 μM forskolin plus 100 nM histamine plus 1 μM clobenpropit are considered 100%. Data are expressed as percentage of control and were analyzed using GraphPad Prism software. Activity at hERG ion channel was determined using Chinese hamster ovary cells stably expressing the channel and an IonWorks recording system (Molecular Devices).

Pharmacokinetics. Male Wistar rats (6–8 weeks old; 200–250 g body weight) were administered a single dose of 5 mg/kg i.v. or 10 mg/kg i.p. SEN12333 at time 0. Levels in plasma were determined over a period of 8 h in the intravenous study and in plasma and brain at 0, 0.5, 1, and 3 h. Concentration of SEN12333 in rat brain and plasma was measured by high-performance liquid chromatography in combination with mass spectrometry (LC-MS/MS), with a limit of detection of 1 ng/ml in plasma and 10 ng/g in brain. Plasma samples were prepared by protein precipitation with acetonitrile containing 250 ng/ml internal standard, centrifugation, and analysis of the supernatant by LC-MS/MS. Brain samples were prepared by homogenization and extraction with methanol. The homogenates were subsequently centrifuged, and the supernatant was analyzed by LC-MS/MS. Quantification was performed in a similar manner to the plasma samples.

Object Recognition Test. Object recognition was evaluated as described previously (Scali et al., 1997) using different amnesic factors. Scopolamine- (0.2 mg/kg i.p.) and MK-801 (0.03 mg/kg i.p.)-induced amnesia was provoked 30 min before acquisition trials, whereas spontaneous decay of memory was induced by the time delay after first experience (24-h time delay). SEN12333 (1–10 mg/kg) was administered 30 min before the acquisition trial to determine whether SEN12333 could reverse the cognitive impairments produced by the amnesic factor.

In brief, for scopolamine and time delay protocols, Wistar rats were placed in a gray polyvinylchloride arena (60 × 60 × 40 cm) illuminated by a 50-W lamp suspended 50 cm above the arena. The objects to be discriminated were prisms, pyramids, and cylinders made of plastic. The day before testing, rats were habituated to the arena for 2 min. In the scopolamine-induced amnesia, a session of two trials separated by an intertrial interval of 240 min was carried out. In the first trial (acquisition trial, T1), two identical objects were presented in two opposite corners of the arena. The rats were left in the arena until criterion of 20 s of total exploration of the objects was reached. Exploration was defined as directing the nose at a distance <2 cm to the object and/or touching it with the nose. During the second trial (retention trial, T2), one of the objects presented in T1 was replaced by a novel object, and rats were left in the arena for 5 min. The time spent exploring the familiar (F) and the novel object (N) was recorded separately, and the difference between the two exploration times was taken. From one rat to the next, care was taken to avoid object and place preference by randomly changing the role of the objects (familiar or new object) and their position in the two opposite corners of the box during T2. Furthermore, to avoid olfactory stimuli the objects to be discriminated were cleaned with a 30% ethanol solution between animals. In the time delay procedure, T2 was performed 24 h after T1 when a spontaneous decay of memory was present in control rats. Student's paired *t* test was used to evaluate differences between exploration time. MK-801-induced novel object recognition deficit was evaluated in a procedure similar

to that used for the scopolamine-induced deficit. Long Evans rats were tested in a circular field (diameter, ~70 cm; height, 30 cm), surrounded by black curtains masking extrafield cues, located in a dimly lit room (~10 lux at the level of the area) in the presence of white noise (~65 dB). Animal performance was tracked by video using EthoVision XT software (Noldus Information Technology, Inc., Leesburg, VA). Objects, constructed with Duplo (Lego, Billund, Denmark), were placed on the arena floor in one of four locations spaced evenly around the field approximately 10 cm from the field's edge. Rats were habituated to the arena that contained two identical yellow cubes for a period of 15 min 1 day before the T1 and T2 sessions. After a 5-min T1 training session, during which rats were placed in the arena containing two identical novel objects located in the same position previously occupied by the yellow cubes, rats were returned to their home cages for a 1-h retention interval and then tested in the T2 trial for recognition memory. T2 consisted of a 5-min exploration of the field containing both a familiar, previously explored object and a novel object. The location of the objects, counterbalanced across treatment groups, remained constant for each animal during the habituation, T1, and T2 trials. The effect of treatment on object exploration during the retention trial was examined using a one-way ANOVA on total contact time followed by Fisher's LSD group mean pairwise comparisons. The amount of time exploring the novel and familiar objects across treatment groups was analyzed using repeated measures ANOVA followed by Fisher's LSD post hoc comparisons.

Passive Avoidance Test. Wistar rats were tested in a two-compartment step-through passive avoidance apparatus (Basile, Milan, Italy) as described previously (Vannucchi et al., 1997), with minor modifications. Habituation was performed for 1 min in the apparatus the day before testing. During the training trial, each rat was placed in the illuminated chamber, and the latency between door opening and entrance in the dark compartment was measured. When the rat entered the dark chamber, a 0.8-mA scrambled shock was delivered through the floor for 4 s. After 30 s, rats were removed from the dark chamber and returned to their home cages. The intensity of the electric shock was selected after establishing the sensitivity threshold that produced a minimum vocalization and jumping response. Saline- or drug-treated animals showed comparable sensitivity to shock. Retesting was performed 24 h after training. The latency to entrance in the dark chamber was recorded, and better performance was indicated by longer retest latencies (up to a maximum of 240 s). Scopolamine and SEN12333 were administered 30 min before the first trial. Statistical analysis was performed using a one-way ANOVA followed by Fisher's LSD comparisons.

PPI of Acoustic Startle Response in Rats. For these studies, male Long Evans rats (250–350 g; Charles River Italica) were used. Antagonism of pharmacologically induced disruption of PPI was determined in test sessions (using SR LAB equipment; San Diego Instruments, San Diego, CA) consisting of 61 total trials with a 15-s intertrial interval. After a 5-min acclimation to a 64-dB background noise, four trial types (120-dB pulse, or a 69-, 74-, or 79-dB prepulse paired with a 120-dB pulse) were presented in a pseudorandom order. SEN12333 was administered 30 min before testing. The disrupting agent apomorphine (0.54 mg/kg s.c.) was administered 15 min after SEN12333. Prepulse inhibition was defined as 100 − [(startle amplitude on prepulse trials/startle amplitude on pulse-alone trials) × 100]. Data from the pulse-alone trials and average PPI values were analyzed using one-way ANOVA followed by a least significant difference post hoc test ($p < 0.05$).

Quisqualic Acid Injection into the Nucleus Basalis Magnocellularis and Drug Treatment. Quisqualic acid was dissolved in phosphate buffer, pH 7.4, at a concentration of 0.12 M, and 0.5 μl of the solution was injected with a Hamilton microsyringe (Hamilton Co., Reno, NV) into the right nucleus basalis magnocellularis (NBM) of Wistar rats under chloral hydrate anesthesia at the following stereotaxic coordinates: AP, −0.2; L, −2.8 from bregma; and H, −7 from the dura (Casamenti et al., 1998). Control animals were sham-operated by inserting the syringe needle at the NBM coordinates without injection of solution. The study was performed for 7 days after surgery. Rats were intraperitoneally administered with SEN12333 at a dose of 3 mg/kg, or saline with two administrations, 24 and 1 h before surgery, and once daily for 7 days after lesioning. Final administration was performed 1 h before sacrifice.

Immunohistochemistry. Under deep chloral hydrate anesthesia, rats were perfused transcardially with ice-cold paraformaldehyde solution (4% in phosphate buffer, pH 7.4). The brains were postfixed for 4 h and cryoprotected in 18% sucrose solution for at least 48 h. Brains were cut in a cryostat throughout the injected area into 30-μm-thick coronal sections and placed in antifreeze solution (phosphate-buffered saline containing 30% ethylene glycol and 30% glycerol) and stored at −20°C until further use for immunohistochemistry, according to the following schedule. Day 1: for detection of cholinergic neurons, the polyclonal antibody raised against the enzyme choline acetyltransferase (ChAT, 1:1000 dilution; Millipore Bioscience Research Reagents, Temecula, CA) was used. The sections were washed in PBS-0.3% Triton X-100 and then incubated free-floating overnight at room temperature with the primary antibody in PBS solution containing 5 mg/ml, 0.3% Triton X-100, and 0.1% sodium azide. Day 2: after washing in PBS, the sections were incubated in biotinylated secondary antibody (1:1000 dilution; Vector Laboratories, Burlingame, CA) and subsequently incubated in avidin-biotin-peroxidase complex (VECTASTAIN, final dilution, 1:500; Vector Laboratories) and stained using diaminobenzidine (DAB) (Vector Laboratories) in the presence of NiCl. DAB-stained slices were examined using a BX40 microscope (Olympus, Milan, Italy) and photographed using a digital camera (DP50; Olympus). ChAT-positive cells were counted under a 10× objective using a calibrated eyepiece grid. Five sections per animals, standardized in anterior-posterior with respect to the injection site and spaced 50 to 100 μm from each other, were analyzed, and all ChAT-positive cells in the NBM were counted. Only positive cells with a diameter greater than 5 μm were counted. The total number of ChAT-positive cells in the quisqualic acid-injected NBM was compared with the contralateral uninjected side. Statistical analysis was performed by means of one-way ANOVA followed by Fisher LSD comparison test.

Results

In Vitro Pharmacology. SEN12333 (WAY-317538) (Fig. 1) was obtained as part of a structure-activity relationship study based on an initial hit identified in a screening program using a functional FLIPR-Ca^{2+} assay and a GH4C1 cell line stably expressing the rat α7 nAChR. The EC_{50} value of SEN12333 measured in this assay was 1.6 ± 0.9 μM, and the E_{max} value was 106% relative to the response obtained with a maximally active concentration of nicotine (10 μM). No activity was measured in native GH4C1 cells not transfected with the receptor. In radioligand binding experiments, SEN12333 displaced the nicotinic agonist [^{3}H]epibatidine from rat α7 nAChR in membranes prepared from GH4C1 cells, with a K_i value of 260 nM (Table 1).

Whole-cell patch-clamp recordings were performed with GH4C1 cells expressing rat α7 receptors. Each cell was exposed to at least one concentration of ACh and a range of concentrations of SEN12333. The results presented in Fig. 2 show a family of current traces generated by application of increasing concentrations of ACh (Fig. 2a) or SEN12333 (Fig. 2b). SEN12333 evoked a rapidly activating and desensitizing inward current. Activated peak currents and maximal total charges were similar to ACh, suggesting that SEN12333 acts as full agonist at the rat α7 nAChR. In this assay, SEN12333 was approximately 2-fold more potent than ACh, displaying an EC_{50} value of 12 μM (Fig. 2c).

TABLE 1

Summary of EC_{50}, IC_{50}, and binding affinity values (K_i) of SEN12333 at different subtypes of rat and human nAChRs and selectivity profile

Results are the means ± S.E.M. of *n* independent experiments. Agonist (EC_{50}) and antagonist (IC_{50}) activities were determined in FLIPR experiments with a double sequential addition protocol as described under *Materials and Methods*. Concentration ranged from 10^{-9} to 10^{-4} M.

Receptor	SEN12333 EC_{50}	SEN12333 IC_{50}/K_i	*n*
		μM	
rα7 (K_i)		0.26 ± 0.03	3
rα7 (FLIPR)	1.6 ± 0.9		4
rα7 (patch clamp)	12		2
Selectivity (FLIPR)			
hα1β1δγ	Inactive	Inactive	3
hα3β2(α5)	Inactive	8.5 ± 3.6	4
hα4β2	Inactive	45% inhibition at 100 μM	3
h5-HT_{3A}	Inactive	Inactive	4
Broad selectivity			
h histamine H3 receptor (IC_{50})		0.103	
hERG		6% inhibition at 1 μM 29% inhibition at 10 μM	

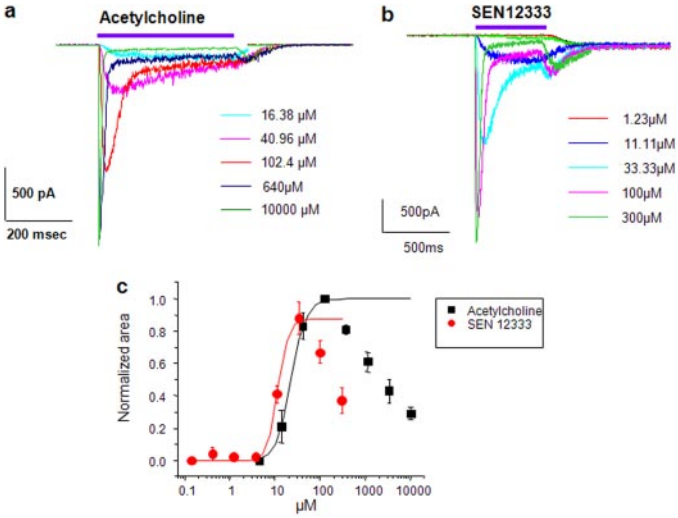

Fig. 2. Electrophysiological characterization of SEN12333 activity at the rat α7 nACh receptor. Whole-cell manual patch-clamp and the Dynaflow rapid perfusion system were used to determine currents evoked by sequential application of ACh (a) or SEN12333 (b), at the indicated concentrations to GH4C1 cells expressing the rat α7 nAChR. Responses from three to four cells were normalized relative to the ACh response and averaged. c, concentration-response curves of SEN12333 and acetylcholine were quantified using total charge area under the curve.

The functional selectivity at different nAChR subtypes and the structurally related 5-HT_{3A} receptor was determined in FLIPR-based Ca^{2+} flux (5-HT_{3A}) or membrane potential assays (α1, α3, and α4β2), depending on the properties of the channel. No significant agonist activity was detected at the human muscle α1β1γδ-nAChR natively expressed in TE671 cells, at the human recombinant α4β2-nAChR, and the human recombinant 5-HT_{3A}R stably expressed in HEK293 cells until the highest concentration tested (100 μM). However, SEN12333 acted as weak antagonist at the human ganglionic α3 nAChR natively expressed in SH-SY5Y cells, with an IC_{50} value of 8.5 μM. Partial inhibition was also observed at the human α4β2 nAChR but only at the highest concentration tested (Table 1).

The selectivity of SEN12333 was further characterized using a panel of 70 binding assays (see *Materials and Methods*). At the tested concentration of 10 μM, SEN12333 showed only negligible affinity to muscarinic, adrenergic, dopamine, adenosine, purine, serotonin, as well as brain and vasoactive intestinal peptide receptors and did not inhibit the activity of acetylcholinesterase. Significant inhibition of binding (72.4%) was only observed for the histamine H3 receptor where SEN12333 acted as functional antagonist (IC_{50} = 103 nM). When tested for activity on hERG, 6% inhibition of this ion channel was determined at a SEN12333 concentration of 1 μM and 29% inhibition at 10 μM.

In Vivo Pharmacology. SEN12333 at the doses used in all experiments was well tolerated and did not affect spontaneous behavior of animals, exploration time, and locomotor activity.

Pharmacokinetic Characteristics. To determine pharmacokinetic properties of SEN12333 and its ability to permeate across the blood-brain barrier, 5 mg/kg i.v. and 10 mg/kg i.p. compound was administered to rats. As shown in Table 2, after intravenous administration, SEN12333 showed a high clearance (43 ml/min/kg), a moderate volume of distribution (2.5 l/kg), and a short elimination half-life (0.8 h). In studies aimed at evaluating the brain penetration after intraperitoneal administration of SEN12333 at the dose of 10 mg/kg, the peak plasma and brain concentrations were measured approximately 30 min after injection. In plasma the maximal

TABLE 2

Summary of rat in vivo pharmacokinetic properties of SEN12333

The table summarizes results obtained from independent studies. A, to determine oral bioavailability of SEN12333, Wistar rats were injected either with 5 mg/kg i.v. or 10 mg/kg p.o., and plasma concentrations of SEN12333 were determined at 10 time intervals up to 24 h (n = 3). B, to determine brain-to-plasma ratio, rats were injected with SEN12333 10 mg/kg i.p., and individual plasma and brain concentrations of SEN12333 were determined after 0.5, 1, and 3 h (n = 3).

	Matrix	Administration Route	Dose	T_{max}	$t_{1/2}$	C_{max}	AUC	Clp	V_{ss}	Brain-Plasma Ratio	F
			mg/kg	*h*	*h*	*Ng/ml*	*h · ng/ml*	*ml/min/kg*	*l/kg*		%
A	Plasma	i.v.	5		0.8	2058	2013	43	2.5		
	Plasma	p.o.	10	0.67	1.5	853	2293				57
B	Plasma	i.p.	10	0.5	0.8	244	347				
	Brain	i.p.	10	0.5	1	644	809			2.5	

Clp, plasma clearance; F, bioavailability; V_{ss}, volume of distribution at steady state.

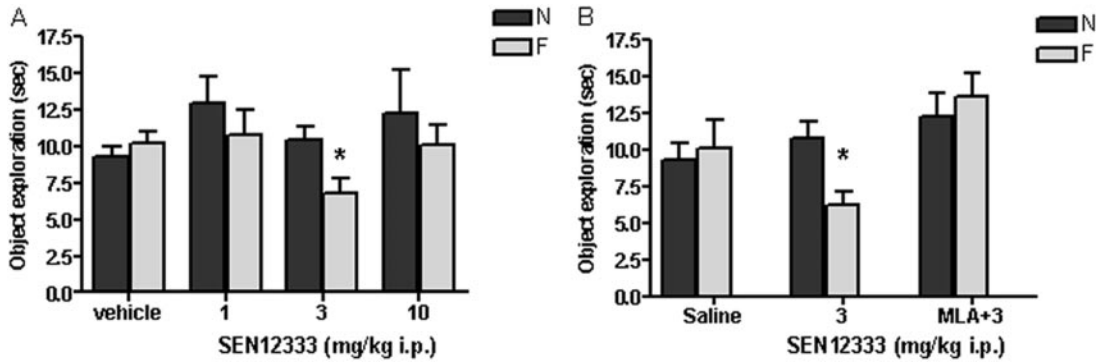

Fig. 3. SEN12333 improves retention in a novel object recognition task using time delay interval as amnesic factor in rats. The positive effect of SEN12333 is reverted by the antagonist MLA. A, SEN12333 was administered intraperitoneally at the indicated doses (1, 3, and 10 mg/kg) 30 min before T1. The interval between the T1 (acquisition) and T2 (retention) trial was 24 h. Bars represent the mean ± S.E.M. time spent exploring an N or an F object during the T2 retention trial. Statistical analysis was performed by Student's paired *t* test (∗, $p < 0.05$ versus respective *F* value; n = 7–12 rats/group). There was no statistically significant effect of treatment on object exploration during the learning phase ($F_{3,35} = 1.31$; $p = 0.32$). B, MLA 5 mg/kg i.p. was administered 5 min before the administration of SEN12333 at the dose of 3 mg/kg i.p. (∗, $p < 0.05$ versus respective *F* value; $n = 6$ rats/group). There was no statistically significant effect of treatment on object exploration during the T1 learning phase ($F_{2,15} = 1.93$; $p = 0.22$).

concentration amounted to 244 ng/ml at this dose, and the half-life was calculated to be between 0.8 and 1 h. The ratio of the amount of compound entering the brain and compound in plasma (AUC_{brain}/AUC_{plasma}) was 2.5, demonstrating good brain penetration in rodents. Additional studies were performed to determine oral bioavailability of SEN12333, which was calculated as F = 57% (Table 2).

Effects on Cognition: Object Recognition Test. The ability of SEN12333 to facilitate episodic memory was evaluated in an object recognition task using different protocols, either a time delay for physiologically occurring amnesia or pharmacologically induced amnesia using scopolamine and MK-801. The mean exploration time during T1 was 1.86 ± 0.21 for vehicle-treated animals. SEN12333, the amnesic agents, and MLA did not influence the exploration time needed to reach the 20-s criterion as demonstrated by the lack of significant difference between groups (see figure legends). In the time delay protocol (Fig. 3), 24 h after the acquisition trial, rats spent an equivalent amount of time investigating a novel and the familiar objects under control conditions (vehicle). Acute administration of a 3 mg/kg i.p. dose of SEN12333 significantly increased the time spent exploring the novel object compared with the familiar objects, whereas the doses of 1 and 10 mg/kg i.p. did not seem to be efficacious. The improvement of object discrimination elicited by SEN12333 was abolished when it was given 5 min after administration of the α7 antagonist MLA (5 mg/kg i.p.) (Fig. 3). MLA alone did not significantly modify the exploration time in these experiments (data not shown).

In the scopolamine-induced amnesia protocol in which novel objects are presented 4 h after exposure to the familiar objects, control rats (treated with vehicle) spent more time exploring the novel object (Fig. 4). Scopolamine (0.2 mg/kg i.p.) administration 30 min before the acquisition trial disrupted the recognition capacity for objects as shown by no significant difference in the amount of time spent exploring the novel or familiar object. Administration of SEN12333 at a dose of 3 mg/kg i.p. restored the preferential investigation of the novel object in scopolamine-treated animals as indicated by the significant difference of the time of exploration ($p < 0.05$). The dose of 10 mg/kg i.p. did not block the cognitive-disrupting effect of scopolamine. When MK-801 was used to induce amnesia, SEN12333 (3 and 10 mg/kg i.p.) again re-established preferential exploration of the novel object comparable with that of vehicle-treated animals (Fig. 5). Reversion of the cognitive deficits induced by MK-801 was also observed in similar experiments that were performed administering SEN12333 orally. Under these conditions, a dose of 10 mg/kg (p.o.) was efficacious, but not 1 and 3 mg/kg (data not shown), demonstrating oral efficacy for SEN12333 in the object recognition task.

Effects on Cognition: Passive Avoidance Test. The passive avoidance test is a well established experimental paradigm for assessment of a form of working memory, short-term reference memory dependent on cortical and hippocampal circuitries. When scopolamine (0.6 mg/kg i.p.) was administered 30 min before the learning trial, it significantly reduced the latency during the retention trial determined 24 h later (Fig. 6). Administration of SEN12333 (1, 3, and 10 mg/kg) together with scopolamine prolonged the latency and reverted the effect of the amnesic drug with a statistically significant effect at 3 mg/kg

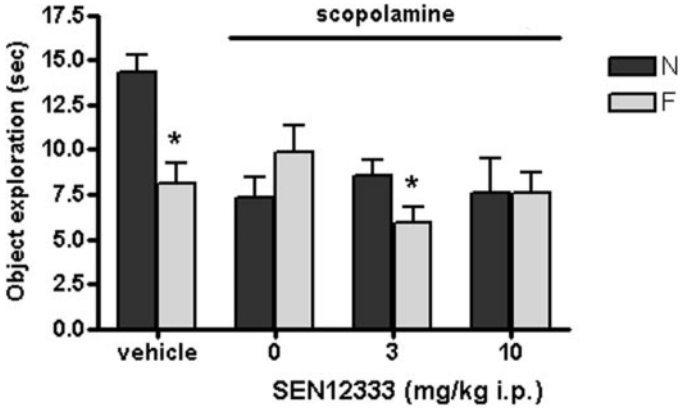

Fig. 4. SEN12333 improves retention in a novel object recognition task using scopolamine as amnesic factor. After the acquisition trial T1, rats were returned to their home cages for a 240-min retention interval and then tested in the choice T2 for recognition memory. SEN12333 (3 and 10 mg/kg i.p.) was administered 5 min before scopolamine (0.2 mg/kg i.p.) and 30 min before T1 to determine whether SEN12333 could reverse the cognitive impairments produced by the muscarinic receptor antagonist. Statistical analysis was performed by Student's paired *t* test (∗, $p < 0.05$ versus respective *F* value; n = 5–10 rats/group; ∗, $p < 0.05$ versus respective *F* value; n = 7–12 rats/group). There was no statistically significant effect of treatment on object exploration during the T1 learning phase ($F_{3,28} = 1.59$; $p = 0.21$).

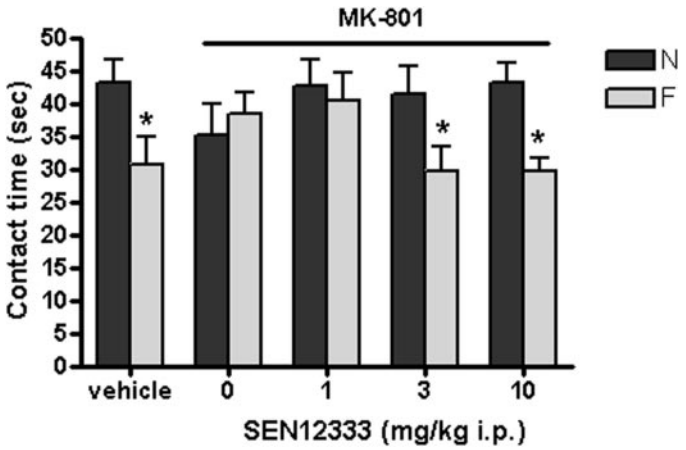

Fig. 5. SEN12333 improves retention in a novel object recognition task using MK-801 as amnesic factor. After the acquisition trial T1, rats were returned to their home cages for a 1-h retention interval and then tested in the choice T2 for recognition memory. SEN12333 (1–10 mg/kg i.p.) and MK-801 (0.03 mg/kg i.p.) were administered 30 min before T1 to determine whether SEN12333 could reverse the cognitive impairments produced by the *N*-methyl-D-aspartate receptor antagonist. The effect of treatment on object exploration during the sample trial was examined using a one-way ANOVA on total contact time followed by Fisher's LSD group mean pairwise comparisons. There was no statistically significant effect of treatment on object exploration during the T1 learning phase ($F_{4,45} = 0.400$; $p = 0.8077$).

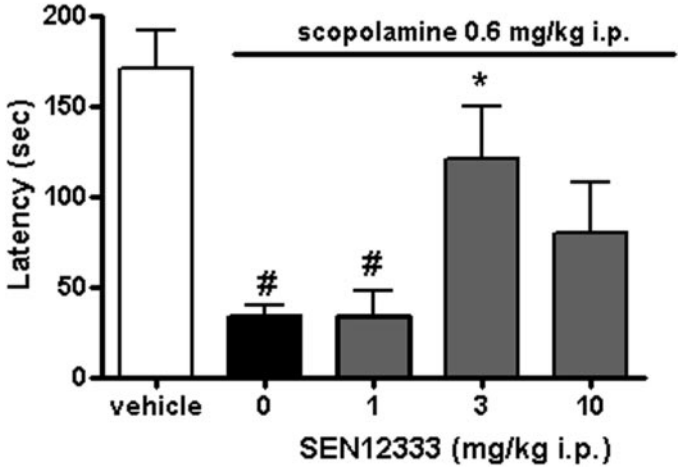

Fig. 6. Effect of SEN12333 administration on passive avoidance test using scopolamine as amnesic factor. SEN12333 at 1, 3, and 10 mg/kg was administered i.p. 30 min before the training trial. Scopolamine (0.6 mg/kg i.p.) was administered 5 min before the administration of SEN12333. Bars represent the mean ± S.E.M. of retest latency measured 24 h after the shock. Statistical analysis was performed by one-way ANOVA ($F_{4,56} = 7.95$; $p < 0.0001$) followed by Fisher's LSD test (*, $p < 0.05$ versus scopolamine; #, $p < 0.05$ versus saline; $n = 8$–15 rats/group).

($p < 0.05$ versus scopolamine). The doses of 1 and 10 mg/kg i.p. were ineffective (Fig. 6).

Effects on Pharmacologically Induced Disruption of PPI. Prepulse inhibition of the acoustic startle response is a behavioral test system to assess preattentive processing that can be disrupted by modulation of the dopaminergic system. Under normal conditions, the presentation of a low level auditory stimulus before a startle-inducing auditory stimulus results in a decrease in startle response relative to the response observed after presentation of the startle stimulus alone. Administration of the dopamine receptor agonist apomorphine (0.54 mg/kg) produced a significant decrease in the ability of a prepulse stimulus to attenuate a startle response. SEN12333 (10 mg/kg i.p.) normalized the apomorphine-induced disruption of PPI (Fig. 7). Analysis revealed a significant treatment effect ($F_{4,34} = 4.47$; $p = 0.0052$) and a prepulse by treatment interaction ($F_{8,68} = 2.29$; $p = 0.0307$). Post hoc comparisons confirmed a significant ($p < 0.05$) apomorphine-induced impairment at all three prepulse intensities and a significant attenuation of the deficit after treatment with 10 mg/kg SEN12333 at the 5-dB prepulse intensity. No significant effect of treatment was observed in the baseline startle response of the animals ($F_{4,34} = 0.531$; $p = 0.7136$) (data not shown).

Neuroprotective Properties Assessed in Vivo. Quisqualic acid-induced lesions of the NBM of rats, in conjunction with determination of ChAT immunoreactivity, is widely used to study cholinergic degeneration in vivo. In a series of experiments, the potential of SEN12333 was evaluated to protect neurons from such degeneration. In control rats (sham-operated), ChAT immunoreactivity in the NBM was localized in intensely labeled magnocellular neurons of oval or triangular shape located at the border between the internal capsule and the globus pallidus (Fig. 8A). Quisqualic acid injection in the NBM induced a massive loss of cholinergic neurons as indicated by 74% decrease in the number of ChAT-immunopositive neurons compared with the uninjected contralateral side. In addition, the surviving neurons revealed shrinkage and loss of projections (Fig. 8, B and D). Subchronic administration of SEN12333 for 7 days significantly attenuated this decrease to approximately 50% (Fig. 8D). Moreover, inspection of the cytological appearance of ChAT-positive neurons revealed an intense labeling of cell bodies that showed better morphology and preserved projections (Fig. 8C).

Discussion

Based on an initial hit identified in a screening program, SEN12333 (WAY-317538) was obtained as the result of a

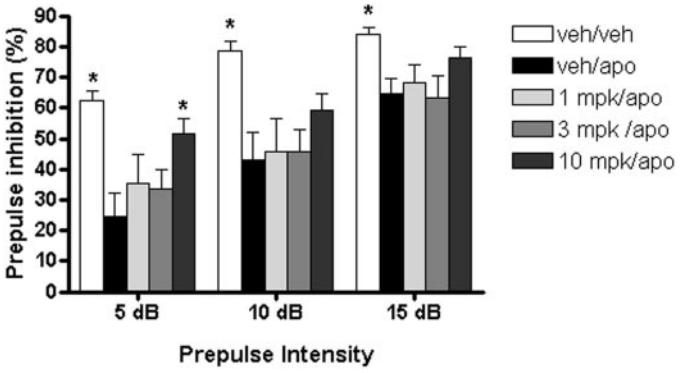

Fig. 7. Normalization of MK-801 disrupted PPI of the acoustic startle response in rats by SEN12333. PPI was measured in male Long-Evans rats ($n = 7$–8/treatment group) as a function of three different prepulse intensities using apomorphine as a pharmacological disruptor. Baseline PPI was significantly attenuated with apomorphine (0.54 mg/kg s.c.; 10-min pretreatment) at all prepulse intensities and SEN12333 (1–10 mg/kg i.p.; 25-min pretreatment) significantly attenuated that disruption at the 5-dB prepulse intensity at the highest dose tested. Data from the pulse-alone trials and average PPI values were analyzed using one-way ANOVA followed by a least significant difference post hoc test [*, $p < 0.05$ versus vehicle/(veh/apo)]. There was no statistically significant effect of treatment on startle response ($F_{4,34} = 0.531$; $p = 0.7136$). veh, vehicle; apo, apomorphine.

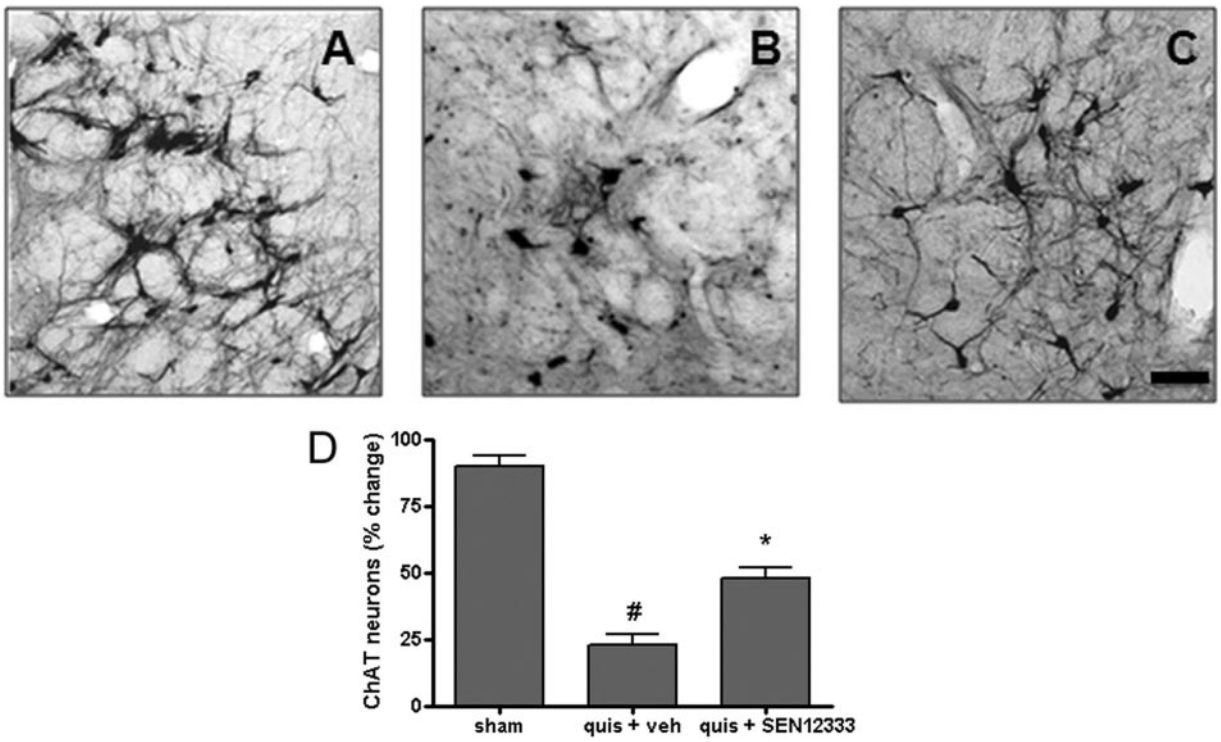

Fig. 8. SEN12333 protects against quisqualic acid-induced degeneration of cholinergic neurons in the NBM of rats. Cholinergic neurons were visualized by immunocytochemistry using polyclonal antibodies against ChAT and DAB staining. Coronal slices in the NBM area were prepared 7 days after surgery and pharmacological treatment with SEN12333. A, sham-operated rats. B, quisqualic acid-injected rats treated with vehicle. C, quisqualic acid-injected rats treated with SEN12333 for 7 days. Scale bar, 50 μm. D, quantitative analysis of ChAT-positive neurons. Bars represent the mean percentage of changes ± S.E.M. in number of ChAT immunoreactive neurons respective to the contralateral side. One-way ANOVA ($F_{2,13} = 36.6$; $p < 0.0001$) followed by Fisher's LSD test (*, $p < 0.05$ versus quisqualic acid-injected + vehicle rats; #, $p < 0.05$ versus sham-operated rats; $n = 4-6$ rats/group).

structure-activity relationship study. SEN12333 binds to the recombinant rat α7 nAChR, with a K_i value of 260 nM, and acts as an agonist, displaying an EC_{50} value of 1.6 μM as measured in a Ca^{2+} flux assay. In whole-cell patch-clamp recordings, SEN12333 activated peak currents and maximal total charges similar to ACh and was therefore classified as full agonist (>80% E_{max} relative to ACh). The functional studies with different cell lines also demonstrated that SEN12333 was selective over related nicotinic receptors: no significant activity was detected at the heteromeric neuronal α4β2 receptor or the muscular receptor. In addition, SEN12333 did not activate the α3β2 nAChR, which represents the ganglionic receptor family, but at this receptor it acted as a weak antagonist (selectivity ratio of 4-fold). Despite the relatively high structural homology of α7 and 5-HT_{3A} receptors, SEN12333 did not significantly activate or block this ion channel, which is in contrast to what has been observed for some other α7 agonists belonging to different chemotypes (Kem, 2000; Broad et al., 2002; Boess et al., 2007). To further characterize the selectivity of SEN12333, its binding to a wide range of receptors was investigated. At a concentration of 10 μM, no detectable inhibition of binding was measured for the neurotransmitter and bioactive peptide receptors tested except for the histamine H3 receptor, where binding was observed leading to receptor antagonism. Inhibition of centrally localized H3 receptors by selective antagonists was shown previously to enhance release of neurotransmitters, suggesting a role for histamine in cognition and H3 receptors as attractive drug targets for the treatment of learning and memory disorders (Esbenshade et al., 2008). In fact, in several preclinical studies H3 antagonists were demonstrated to exert cognition-enhancing effects across multiple cognitive domains (Esbenshade et al., 2008). Therefore, H3 receptor antagonism by SEN12333 would not compromise its potential clinical application

In a series of experiments aimed at the investigation of cognition-enhancing properties of SEN12333, several different rat models were used to test different types of memory deficits known to be affected in AD and schizophrenia. The ability of SEN12333 to improve episodic memory was analyzed in novel object recognition tasks after a period of natural or pharmacologically induced amnesia in rats. This test system is based on the spontaneous exploration behavior of rodents that spend more time with a novel object compared with a familiar object explored before. After a period of 24 h after a first exploration, rats do not retain memory of the objects. When administered acutely, SEN12333 improved performance in both a spontaneous memory paradigm and a short-term episodic memory task in which rats were "impaired" with muscarinic (scopolamine) or glutamatergic *N*-methyl-D-aspartate receptor (MK-801) antagonists. Thus, SEN12333 was able to improve the natural memory and also to compensate for deficits in the cholinergic and glutamatergic systems, which reflect, at least in part, deficits present in patients suffering from Alzheimer's disease. The effects of SEN12333 were also tested on working memory using a passive avoidance test. Administration of the compound significantly prolonged the "step-through" latency in the retention trial in scopolamine-treated rats. The dependence of the observed procognitive effects of SEN12333 from α7 nAChR

activation was demonstrated in the model of spontaneous memory decay in which no additional drugs are used. In this paradigm, the positive effects of SEN12333 were suppressed in the presence of MLA, which is a potent and selective blocker of α7 nAChRs.

The behavioral effects of treatment with SEN12333 in the assays of cognitive function are frequently in the form of an "inverted-U," with efficacy decreasing or no longer evident with increased dose levels. This type of relationship has been described previously for cognitive enhancers acting on the cholinergic system such as acetylcholinesterase inhibitors and nicotine (Lanni et al., 2008) and other nootropic drugs (Bartolini et al., 1996) Modulation of complex synaptic mechanisms and neural circuits, which would need detailed studies to be completely understood, might underlie this phenomenon.

The beneficial in vivo effects of SEN12333 show a profile that is relevant for potential therapy of cognitive deficits observed in AD patients. Such deficits constitute also a significant component in schizophrenia. In fact, deteriorations in schizophrenic patients include episodic, working, and sequential memory, in addition to attentional disturbances and information-processing deficits. When SEN12333 was investigated in a rat model of preattentive processing (prepulse inhibition), it attenuated an apomorphine-induced deficit in this paradigm, providing evidence for the compound's potential to affect sensory processing known to be deficient in schizophrenic patients. Although the effect of SEN12333 is limited to a single prepulse level, the statistical analysis indicates that the effect at 10 mg/kg (post hoc $p = 0.0445$) is significant when analyzed across all prepulse intensities as evidenced by the overall treatment effect ($F_{4,34} = 4.472$; $p = 0.0052$). Given that the effect at this dose may be at a threshold for detection in this model, it is not surprising that an effect would first be evidenced at the 5-dB prepulse intensity (when analyzed at individual prepulse levels). This is likely because of the minimal difference between the background noise and the 5-dB prepulse signal, which should make any disruption the most sensitive to pharmacological reversal.

The results obtained with SEN12333 are in good agreement with observations reported for other recently discovered α7 nAChR agonists that were shown to be efficacious in a variety of in vivo model systems addressing learning and memory as well as attention deficits. For example, AR-R17779 was demonstrated to improve learning in a radial-arm maze (Levin et al., 1999), and *N*-[(3*R*)-1-azabicyclo[2.2.2]oct-3-yl]-7-[2-(methoxy)phenyl]-1-benzofuran-2-carboxamide was efficacious in a social recognition memory test (Boess et al., 2007). PNU282987 and PHA-709829 corrected auditory gating deficits produced by amphetamine in rodents (Hajós et al., 2005; Acker et al., 2008), and SSR-180711 reversed a MK-801-induced deficit in retention of episodic memory in rats (Pichat et al., 2007). MEM-3454 (Rezvani et al., 2009) is currently the most advanced α7 subtype-selective agonist, and proof-of-concept was recently demonstrated by the positive outcome of a phase II clinical trial for mild-to-moderate AD. This compound has a statistically significant effect on quality of episodic secondary memory, a composite score derived from memory tests in the cognitive drug research battery (Memory Pharmaceutical Communication, 2007). Cumulatively, the results obtained with several different α7 subtype-selective nAChR agonists clearly demonstrate the therapeutic value of modulating this target for treatment of disorders associated with cognitive deficits such as AD.

In addition to amyloid plaques and tangles, loss of cholinergic neurons in the basal forebrain nuclei and concomitant cholinergic hypofunction is another prominent neuropathological feature of AD (Bartus et al., 1982). A useful model system mimicking such cholinergic hypofunction was demonstrated to be excitotoxin-induced lesion of the NBM with quisqualic acid, which results in a more selective destruction of cholinergic neurons in the basal forebrain compared with other excitotoxic amino acids (Casamenti et al., 1998). To investigate the neuroprotective properties of SEN12333, a unilateral lesion with quisqualic acid in the NBM of adult rats was generated. Animals were then subjected to subchronic treatment for 7 days after lesion with a dose of SEN12333 (3 mg/kg i.p.) that was efficacious in the behavioral test systems. This treatment significantly reduced the level of degeneration of cholinergic neurons as demonstrated by an increased number of ChAT-positive neurons and a better preservation of neuronal morphology in comparison with lesioned animals that did not receive SEN12333 treatment. These in vivo results are very important because they provide evidence for a potential role of α7 nAChR agonists in neurodegeneration thus going beyond symptomatic therapy toward disease modification in AD. Previously, protective effects have been demonstrated in several studies with nicotine. Because nicotine is a broad-spectrum agonist of nAChR, discrimination of the receptor(s) underlying the observed protection was limited to use of specific antagonists. More recently, some of the identified more selective α7 nAChR agonists were also tested against a variety of toxic insults, and some of them were shown to be protective. However, because these studies have been conducted in vitro using cell lines of neuronal origin or primary neurons in culture, their pharmacological relevance is limited. To date, only very few reports exist describing effects of α7 nAChR agonists in neurodegenerative models in vivo. One such study showed that chronic treatment with the anabasine derivative 3-(4-hydroxy, 2-methoxybenzylidene)anabaseine was able to protect against loss and atrophy of axotomized septal cholinergic neurons, although a similar positive effect was not observed in PS1 or APP/PS1 transgenic mice (Ren et al., 2007). The authors proposed that either a direct effect of α7 nAChR activation or an indirect effect through increased nerve growth factor release or elevated trkA receptor levels were responsible for the observed protection.

A further component that might be associated with α7 nAChR-dependent neuroprotection may be related to modifications of neuroinflammatory processes occurring upon neuronal damage. This hypothesis is supported by the recent identification of α7 AChR expression in peripheral macrophages, which operate the so-called "cholinergic anti-inflammatory pathway" regulating systemic inflammatory responses in the peripheral nervous system (Wang et al., 2003), and murine microglia, which is involved in suppression of neuroinflammation (Shytle et al., 2004; De Simone et al., 2005). In fact, in microglia activation of α7 AChRs seemed capable of changing the activity from an overactive inflammatory to a protective cell type (Suzuki et al., 2006), further corroborating an important role of α7 AChRs in neuroprotection. More specific studies, which are outside the scope of the current pharmacological characterization, are necessary to

determine the mechanism(s) by which α7 nAChR activation with SEN12333 leads to reduced neuronal damage caused by excitotoxic insult to neurons. Moreover, the relevance of these findings for neurodegenerative disorders such as AD need to be investigated further and whether neuroprotective effects mediated through α7 nAChR activation can be translated into clinical benefits for patients.

In summary, the results presented here demonstrate that the novel α7 agonist SEN12333 elicits wide-ranging efficacy across different cognitive domains relevant to pathologies such as AD and schizophrenia. Based on its neuroprotective properties, SEN12333 might also alter the process of neurodegenerative diseases such as AD, leading to disease modification.

Acknowledgments

We thank Michele Guerrini for excellent technical assistance and animal care as well as Flora Jow, Tim Lock, and Angela Kramer for excellent technical contribution to this study.

References

Acker BA, Jacobsen EJ, Rogers BN, Wishka DG, Reitz SC, Piotrowski DW, Myers JK, Wolfe ML, Groppi VE, Thornburgh BA, et al. (2008) Discovery of *N*-[(3*R*,5*R*)-1-azabicyclo[3.2.1]oct-3-yl]furo[2,3-*c*]pyridine-5-carboxamide as an agonist of the alpha7 nicotinic acetylcholine receptor: in vitro and in vivo activity. *Bioorg Med Chem Lett* **18:**3611–3615.

Alkondon M, Pereira EF, Eisenberg HM, and Albuquerque EX (2000) Nicotinic receptor activation in human cerebral cortical interneurons: a mechanism for inhibition and disinhibition of neuronal networks. *J Neurosci* **20:**66–75.

Bartolini L, Casamenti F, and Pepeu G (1996) Aniracetam restores object recognition impaired by age, scopolamine, and nucleus basalis lesions. *Pharmacol Biochem Behav* **53:**277–283.

Bartus RT, Dean RL 3rd, Beer B, and Lippa AS (1982) The cholinergic hypothesis of geriatric memory dysfunction. *Science* **217:**408–414.

Boess FG, De Vry J, Erb C, Flessner T, Hendrix M, Luithle J, Methfessel C, Riedl B, Schnizler K, van der Staay FJ, et al. (2007) The novel α7 nicotinic acetylcholine receptor agonist *N*-[(3*R*)-1-azabicyclo[2.2.2]oct-3-yl]-7-[2-(methoxy)phenyl]-1-benzofuran-2-carboxamide improves working and recognition memory in rodents. *J Pharmacol Exp Ther* **321:**716–725.

Broad LM, Felthouse C, Zwart R, McPhie GI, Pearson KH, Craig PJ, Wallace L, Broadmore RJ, Boot JR, Keenan M, et al. (2002) PSAB-OFP, a selective alpha 7 nicotinic receptor agonist, is also a potent agonist of the 5-HT3 receptor. *Eur J Pharmacol* **452:**137–144.

Casamenti F, Prosperi C, Scali C, Giovannelli L, and Pepeu G (1998) Morphological, biochemical and behavioural changes induced by neurotoxic and inflammatory insults to the nucleus basalis. *Int J Dev Neurosci* **16:**705–714.

Counts SE, He B, Che S, Ikonomovic MD, DeKosky ST, Ginsberg SD, and Mufson EJ (2007) alpha7 Nicotinic receptor up-regulation in cholinergic basal forebrain neurons in Alzheimer disease. *Arch Neurol* **64:**1771–1776.

Court J, Martin-Ruiz C, Piggott M, Spurden D, Griffiths M, and Perry E (2001) Nicotinic receptor abnormalities in Alzheimer's disease. *Biol Psychiatry* **49:**175–184.

De Simone R, Ajmone-Cat MA, Carnevale D, and Minghetti L (2005) Activation of alpha7 nicotinic acetylcholine receptor by nicotine selectively up-regulates cyclooxygenase-2 and prostaglandin E2 in rat microglial cultures. *J Neuroinflammation* **2:**4.

Dunlop J, Roncarati R, Jow B, Bothmann H, Lock T, Kowal D, Bowlby M, and Terstappen GC (2007) In vitro screening strategies for nicotinic receptor ligands. *Biochem Pharmacol* **74:**1172–1181.

Esbenshade TA, Browman KE, Bitner RS, Strakhova M, Cowart MD, and Brioni JD (2008) The histamine H3 receptor: an attractive target for the treatment of cognitive disorders. *Br J Pharmacol* **154:**1166–1181.

Fabian-Fine R, Skehel P, Errington ML, Davies HA, Sher E, Stewart MG, and Fine A (2001) Ultrastructural distribution of the alpha7 nicotinic acetylcholine receptor subunit in rat hippocampus. *J Neurosci* **21:**7993–8003.

Frazier CJ, Rollins YD, Breese CR, Leonard S, Freedman R, and Dunwiddie TV (1998) Acetylcholine activates an alpha-bungarotoxin-sensitive nicotinic current in rat hippocampal interneurons, but not pyramidal cells. *J Neurosci* **18:**1187–1195.

Freedman R, Adams CE, and Leonard S (2000) The alpha7-nicotinic acetylcholine receptor and the pathology of hippocampal interneurons in schizophrenia. *J Chem Neuroanat* **20:**299–306.

Gault J, Hopkins J, Berger R, Drebing C, Logel J, Walton C, Short M, Vianzon R, Olincy A, Ross RG, et al. (2003) Comparison of polymorphisms in the alpha7 nicotinic receptor gene and its partial duplication in schizophrenic and control subjects. *Am J Med Genet B Neuropsychiatr Genet* **123B:**39–49.

Gotti C and Clementi F (2004) Neuronal nicotinic receptors: from structure to pathology. *Prog Neurobiol* **74:**363–396.

Gotti C, Zoli M, and Clementi F (2006) Brain nicotinic acetylcholine receptors: native subtypes and their relevance. *Trends Pharmacol Sci* **27:**482–491.

Hajós M, Hurst RS, Hoffmann WE, Krause M, Wall TM, Higdon NR, and Groppi VE (2005) The selective α7 nicotinic acetylcholine receptor agonist PNU-282987 [*N*-[(3*R*)-1-azabicyclo[2.2.2]oct-3-yl]-4-chlorobenzamide hydrochloride] enhances GABAergic synaptic activity in brain slices and restores auditory gating deficits in anesthetized rats. *J Pharmacol Exp Ther* **312:**1213–1222.

Hellström-Lindahl E, Court J, Keverne J, Svedberg M, Lee M, Marutle A, Thomas A, Perry E, Bednar I, and Nordberg A (2004) Nicotine reduces A beta in the brain and cerebral vessels of APPsw mice. *Eur J Neurosci* **19:**2703–2710.

Hu M, Schurdak ME, Puttfarcken PS, El Kouhen R, Gopalakrishnan M, and Li J (2007) High content screen microscopy analysis of A beta 1-42-induced neurite outgrowth reduction in rat primary cortical neurons: neuroprotective effects of alpha 7 neuronal nicotinic acetylcholine receptor ligands. *Brain Res* **1151:**227–235.

Jessen F, Kucharski C, Fries T, Papassotiropoulos A, Hoenig K, Maier W, and Heun R (2001) Sensory gating deficit expressed by a disturbed suppression of the P50 event-related potential in patients with Alzheimer's disease. *Am J Psychiatry* **158:**1319–1321.

Kem WR (2000) The brain alpha7 nicotinic receptor may be an important therapeutic target for the treatment of Alzheimer's disease: studies with DMXBA (GTS-21). *Behav Brain Res* **113:**169–181.

Kihara T, Shimohama S, Sawada H, Honda K, Nakamizo T, Shibasaki H, Kume T, and Akaike A (2001) α7 Nicotinic receptor transduces signals to phosphatidylinositol 3-kinase to block A β-amyloid-induced neurotoxicity. *J Biol Chem* **276:**13541–13546.

Lanni C, Lenzken SC, Pascale A, Del Vecchio I, Racchi M, Pistoia F, and Govoni S (2008) Cognition enhancers between treating and doping the mind. *Pharmacol Res* **57:**196–213.

Levin ED, Bettegowda C, Blosser J, and Gordon J (1999) AR-R17779, and alpha7 nicotinic agonist, improves learning and memory in rats. *Behav Pharmacol* **10:**675–680.

Marchi M, Risso F, Viola C, Cavazzani P, and Raiteri M (2002) Direct evidence that release-stimulating alpha7* nicotinic cholinergic receptors are localized on human and rat brain glutamatergic axon terminals. *J Neurochem* **80:**1071–1078.

Newhouse PA, Potter A, and Singh A (2004) Effects of nicotinic stimulation on cognitive performance. *Curr Opin Pharmacol* **4:**36–46.

O'Neill MJ, Murray TK, Lakics V, Visanji NP, and Duty S (2002) The role of neuronal nicotinic acetylcholine receptors in acute and chronic neurodegeneration. *Curr Drug Targets CNS Neurol Disord* **1:**399–411.

Pichat P, Bergis OE, Terranova JP, Urani A, Duarte C, Santucci V, Gueudet C, Voltz C, Steinberg R, Stemmelin J, et al. (2007) SSR180711, a novel selective alpha7 nicotinic receptor partial agonist: (II) efficacy in experimental models predictive of activity against cognitive symptoms of schizophrenia. *Neuropsychopharmacology* **32:**17–34.

Ren K, King MA, Liu J, Siemann J, Altman M, Meyers C, Hughes JA, and Meyer EM (2007) The alpha7 nicotinic receptor agonist 4OH-GTS-21 protects axotomized septohippocampal cholinergic neurons in wild type but not amyloid-overexpressing transgenic mice. *Neuroscience* **148:**230–237.

Rezvani AH, Kholdebarin E, Brucato FH, Callahan PM, Lowe DA, and Levin ED (2009) Effect of R3487/MEM3454, a novel nicotinic α7 receptor partial agonist and 5-HT3 antagonist on sustained attention in rats. *Prog Neuropsychopharmacol Biol Psychiatry* **33:**269–275.

Scali C, Giovannini MG, Prosperi C, Bartolini L, and Pepeu G (1997) Tacrine administration enhances extracellular acetylcholine in vivo and restores the cognitive impairment in aged rats. *Pharmacol Res* **36:**463–469.

Shytle RD, Mori T, Townsend K, Vendrame M, Sun N, Zeng J, Ehrhart J, Silver AA, Sanberg PR, and Tan J (2004) Cholinergic modulation of microglial activation by alpha 7 nicotinic receptors. *J Neurochem* **89:**337–343.

Stassen HH, Bridler R, Hägele S, Hergersberg M, Mehmann B, Schinzel A, Weisbrod M, and Scharfetter C (2000) Schizophrenia and smoking: evidence for a common neurobiological basis? *Am J Med Genet* **96:**173–177.

Suzuki T, Hide I, Matsubara A, Hama C, Harada K, Miyano K, Andrä M, Matsubayashi H, Sakai N, Kohsaka S, et al. (2006) Microglial alpha7 nicotinic acetylcholine receptors drive a phospholipase C/IP3 pathway and modulate the cell activation toward a neuroprotective role. *J Neurosci Res* **83:**1461–1470.

Teaktong T, Graham A, Court J, Perry R, Jaros E, Johnson M, Hall R, and Perry E (2003) Alzheimer's disease is associated with a selective increase in alpha7 nicotinic acetylcholine receptor immunoreactivity in astrocytes. *Glia* **41:**207–211.

Van Kampen M, Selbach K, Schneider R, Schiegel E, Boess F, and Schreiber R (2004) AR-R 17779 improves social recognition in rats by activation of nicotinic alpha7 receptors. *Psychopharmacology (Berl)* **172:**375–383.

Vannucchi MG, Scali C, Kopf SR, Pepeu G, and Casamenti F (1997) Selective muscarinic antagonists differentially affect in vivo acetylcholine release and memory performances of young and aged rats. *Neuroscience* **79:**837–846.

Wang H, Yu M, Ochani M, Amella CA, Tanovic M, Susarla S, Li JH, Wang H, Yang H, Ulloa L, et al. (2003) Nicotinic acetylcholine receptor alpha7 subunit is an essential regulator of inflammation. *Nature* **421:**384–388.

Yu WF, Guan ZZ, Bogdanovic N, and Nordberg A (2005) High selective expression of alpha7 nicotinic receptors on astrocytes in the brains of patients with sporadic Alzheimer's disease and patients carrying Swedish APP 670/671 mutation: a possible association with neuritic plaques. *Exp Neurol* **192:**215–225.

Address correspondence to: Dr. Renza Roncarati, Strada del Petriccio e Belriguardo, 35, 53100 Siena, Italy. E-mail: rroncarati@sienabiotech.it